

## Supplementary Material

### Osmium (II) polypyridyl probe with a therapeutic twist: disrupting the mitochondrial membrane potential for targeted therapy

Karmel Sofia Gkika, Aisling Byrne and Tia E. Keyes

#### <sup>1</sup>H NMR spectra of tpybenzCOOH and Os(II) complexes

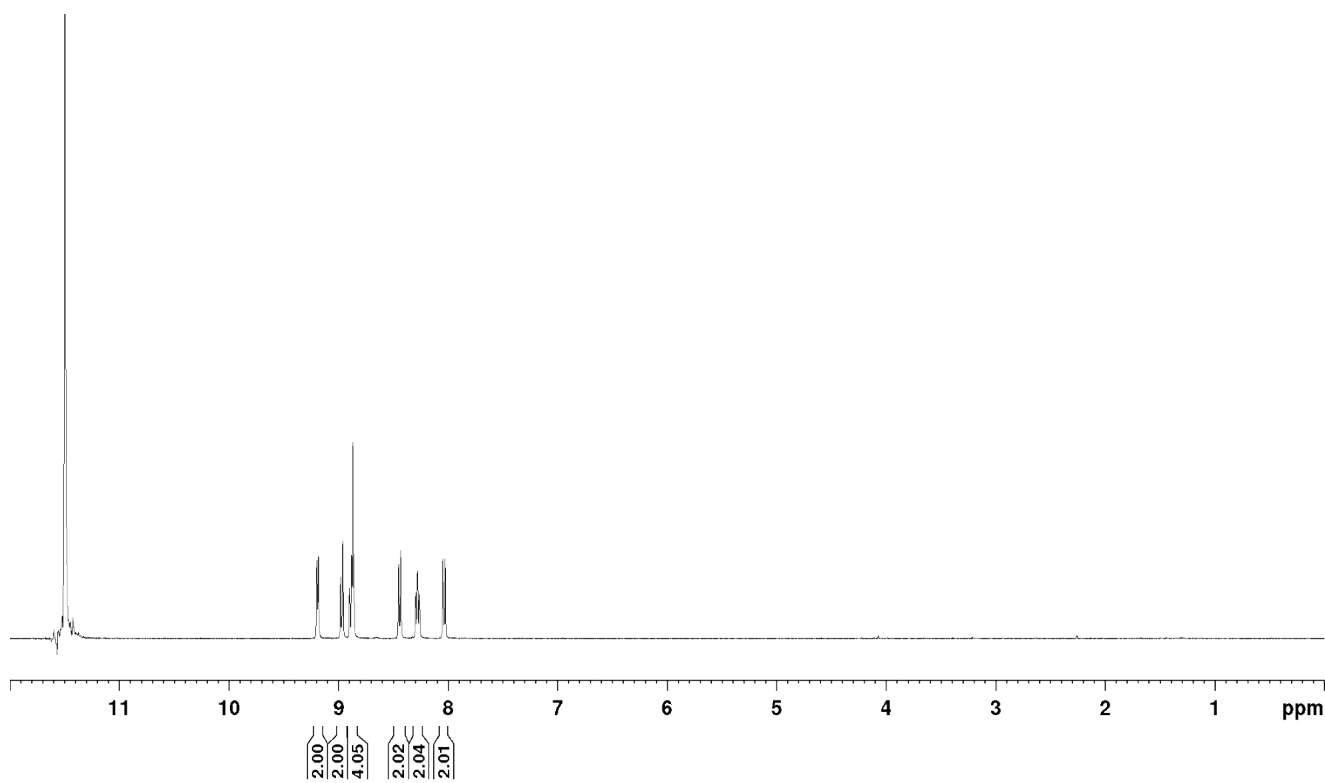


Figure S1: <sup>1</sup>H-NMR spectra of tpybenzCOOH in DMSO-d<sub>6</sub> (top) and TFA-d, (bottom) 600 MHz

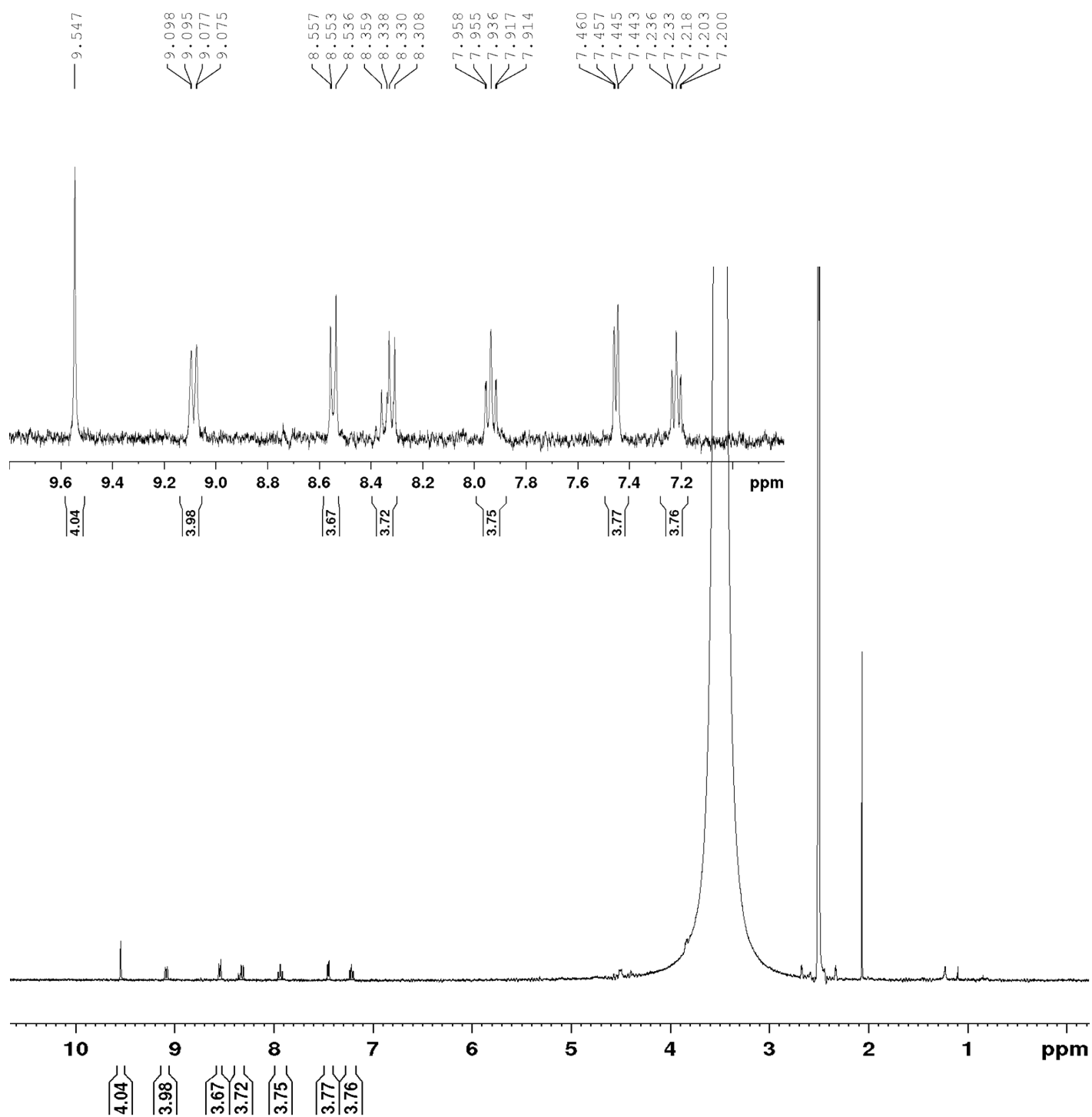


Figure S2:  $^1\text{H}$  NMR of purified  $[\text{Os}(\text{tpybenzCOOH})_2]^{2+}$  in  $\text{DMSO-d}_6$ , 400 MHz

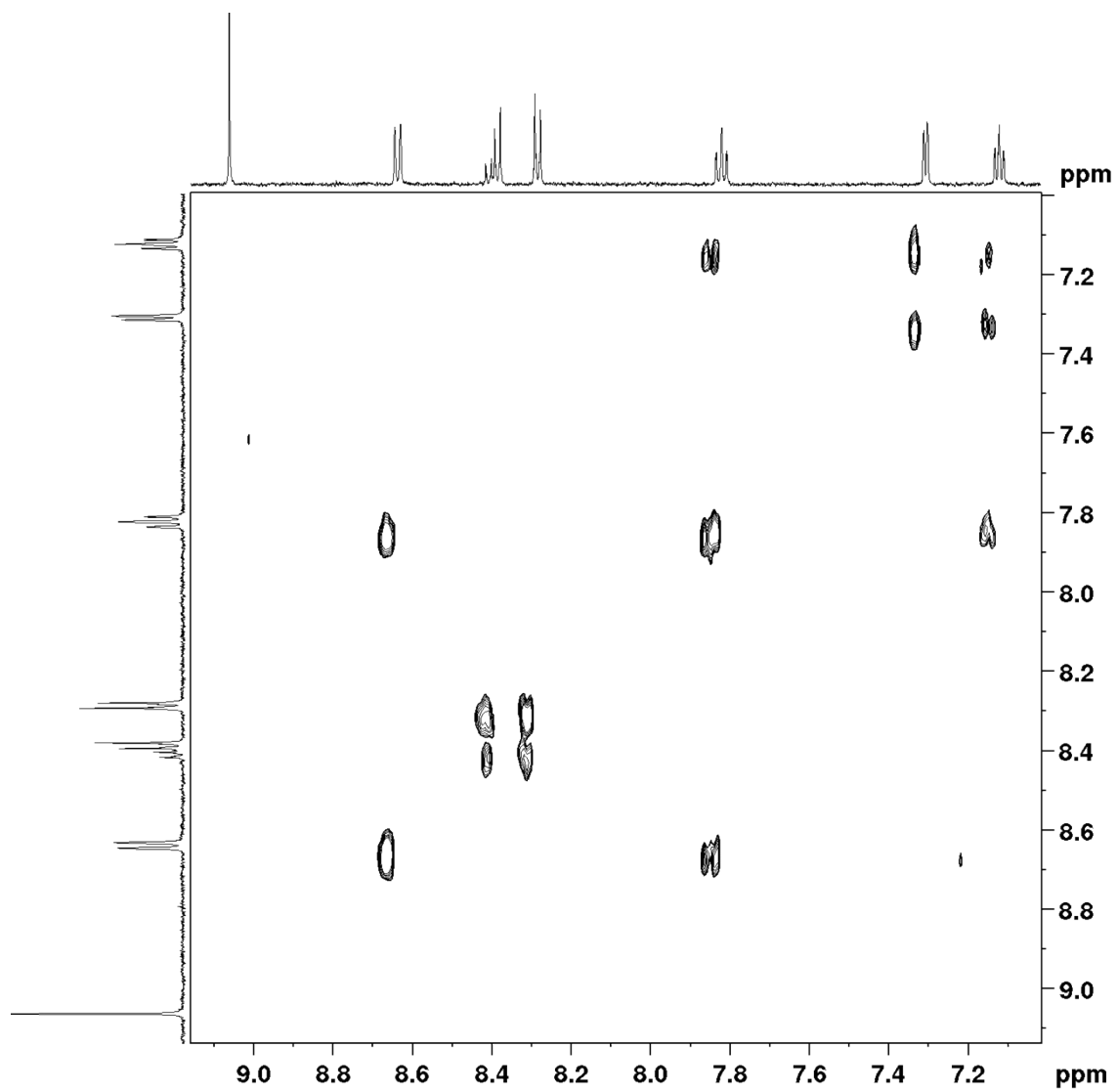


Figure S3: COSY spectrum of  $[\text{Os}(\text{tpybenzCOOH})_2]^{2+}$  in  $\text{MeCN-d}_3$ , 600 MHz

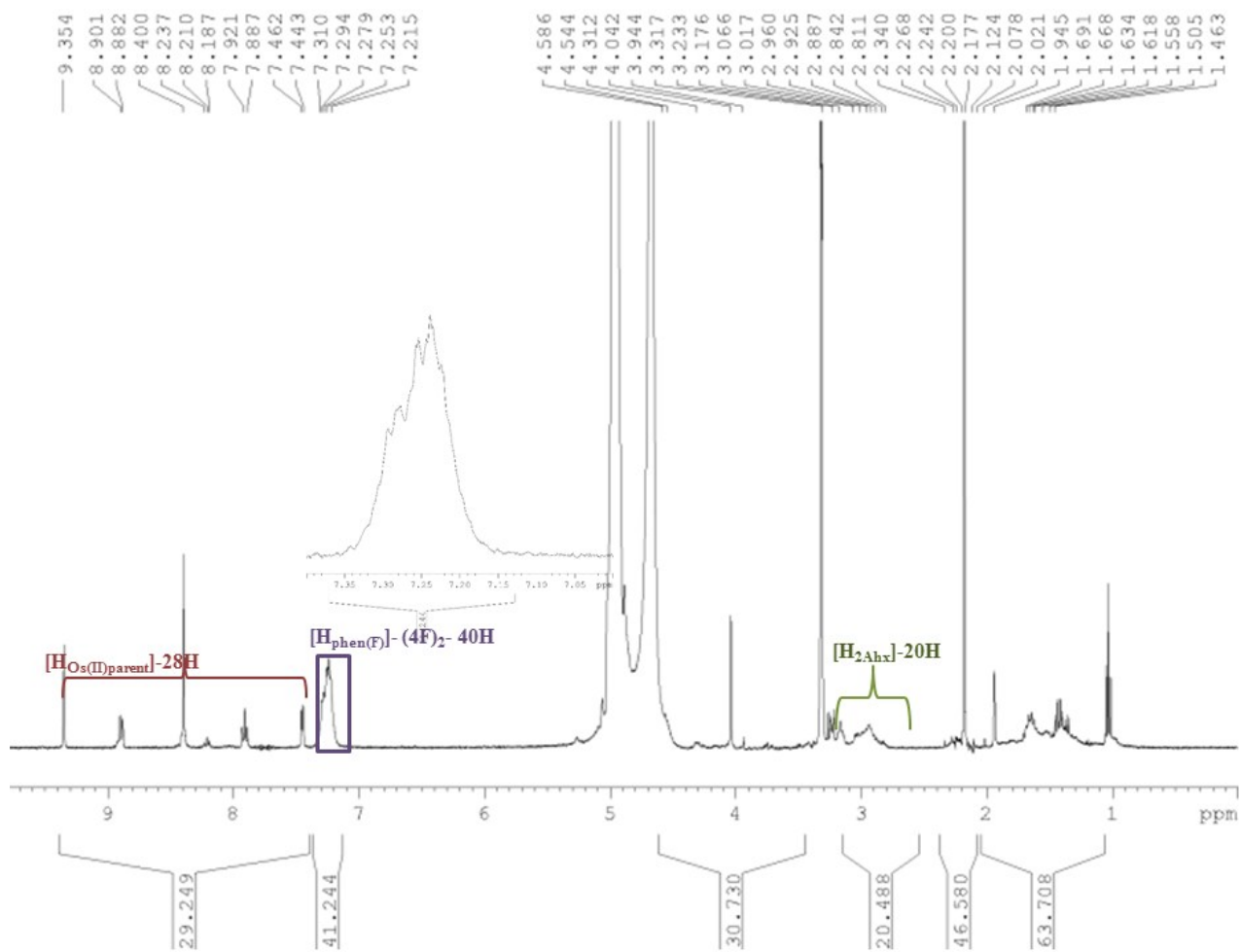


Figure S4:  $^1H$  NMR spectrum of  $Os^{II}MPP$  in  $MeOH-d_4$ , 400 MHz with key regions in the aromatic and aliphatic region highlighted

## Mass Spectrometry Analysis

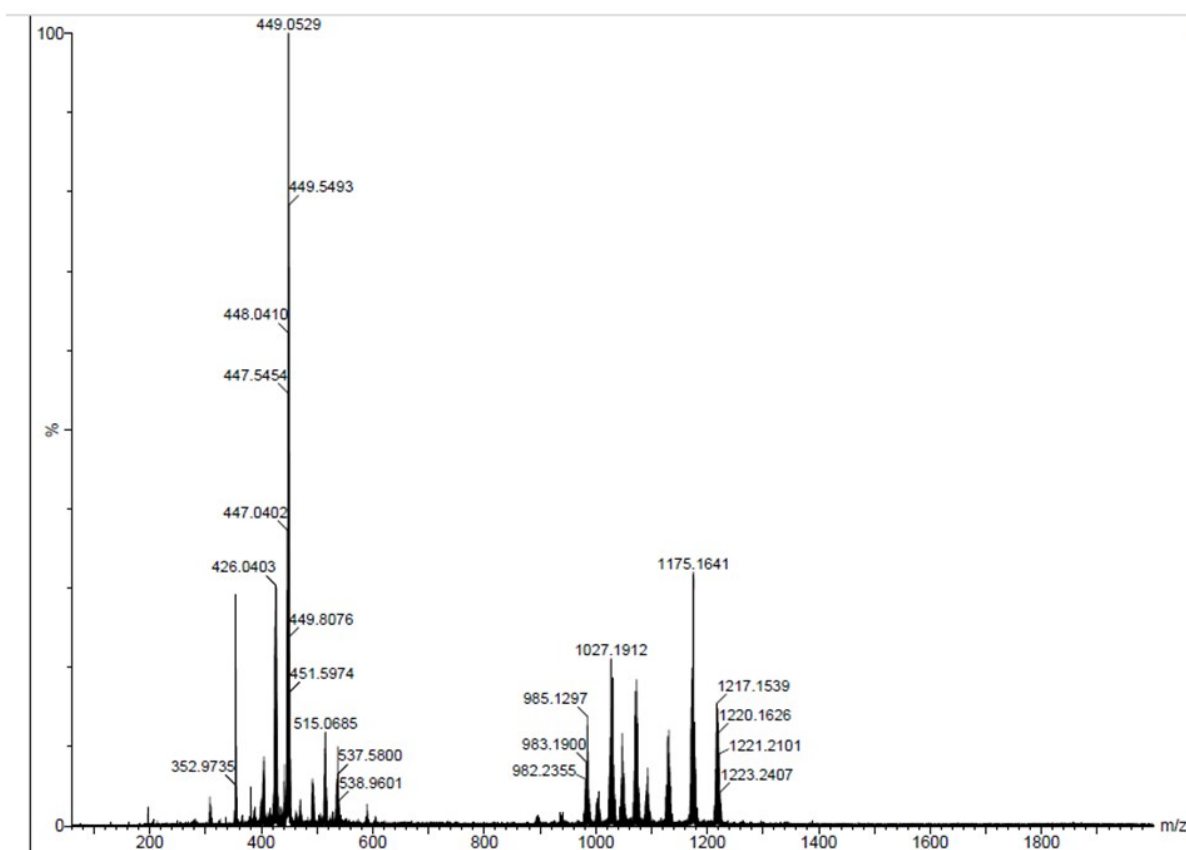
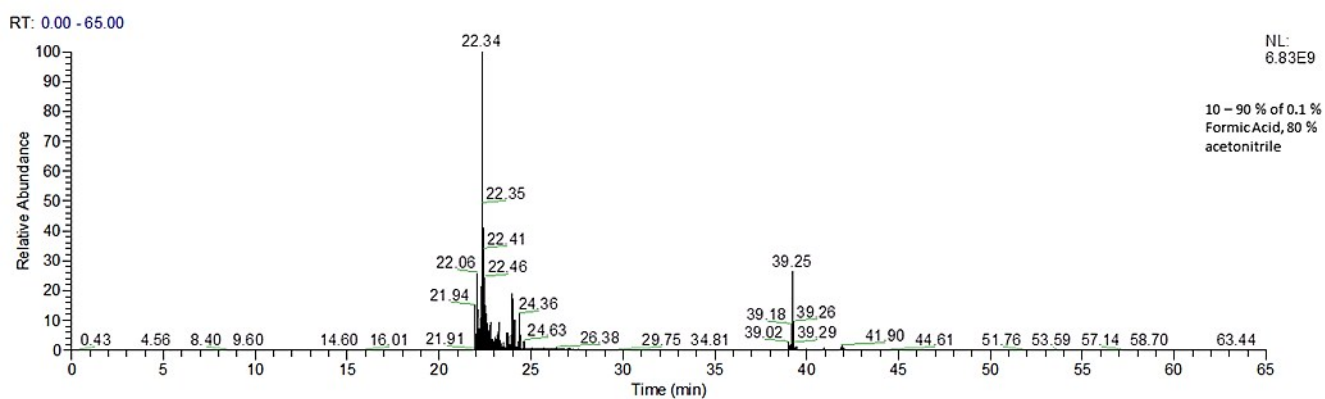


Figure S5: HRMS (TOF ES+) of  $[\text{Os}(\text{tpybenzCOOH})_2]^{2+}$



Blank\_6 #5550-6384 RT: 22.75-24.81 AV: 215 NL: 8.44E7  
 T: FTMS + p NSI Full ms [400.0000-1600.0000]

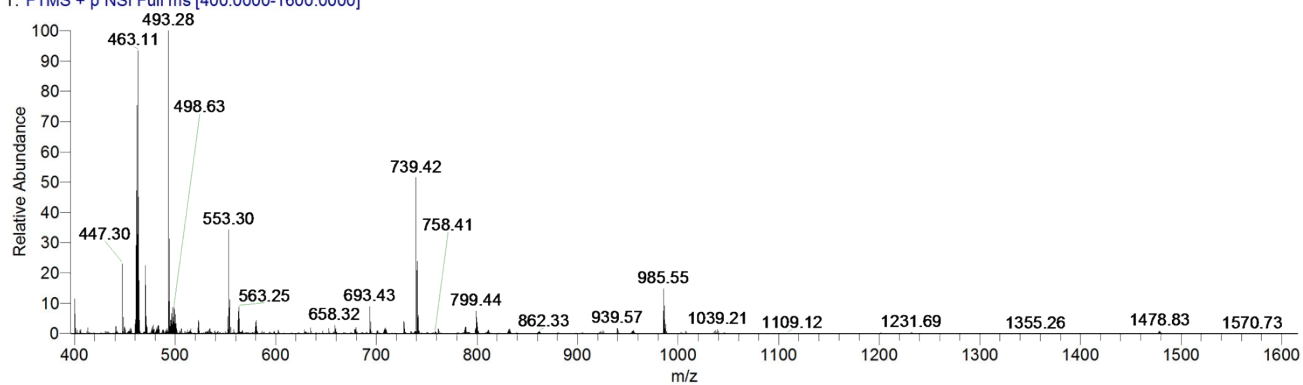


Figure S6: HPLC chromatogram (above) and Mass Spectrum (below) of Os<sup>II</sup> MPP complex following LC-MS analysis (Q-Exactive). Conditions; gradient extended from 10- 90% (Formic Acid 0.1%, 80% MeCN).

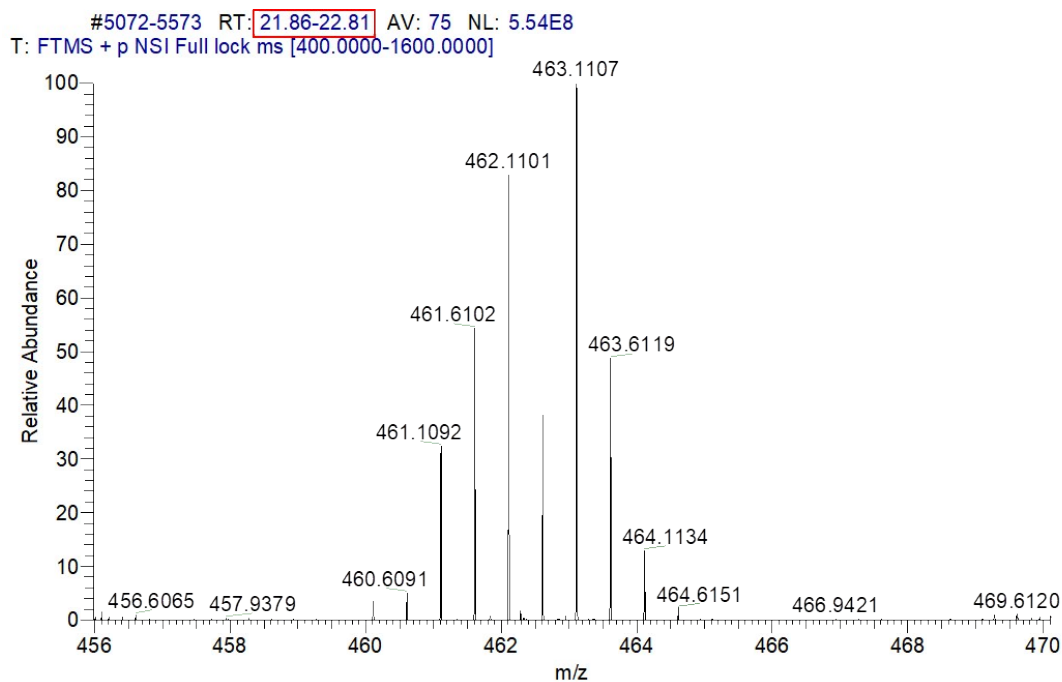


Figure S7: LC-MS analysis of Os<sup>II</sup>MPP Zoomed m/z 456-470 (RT 21-23 min)

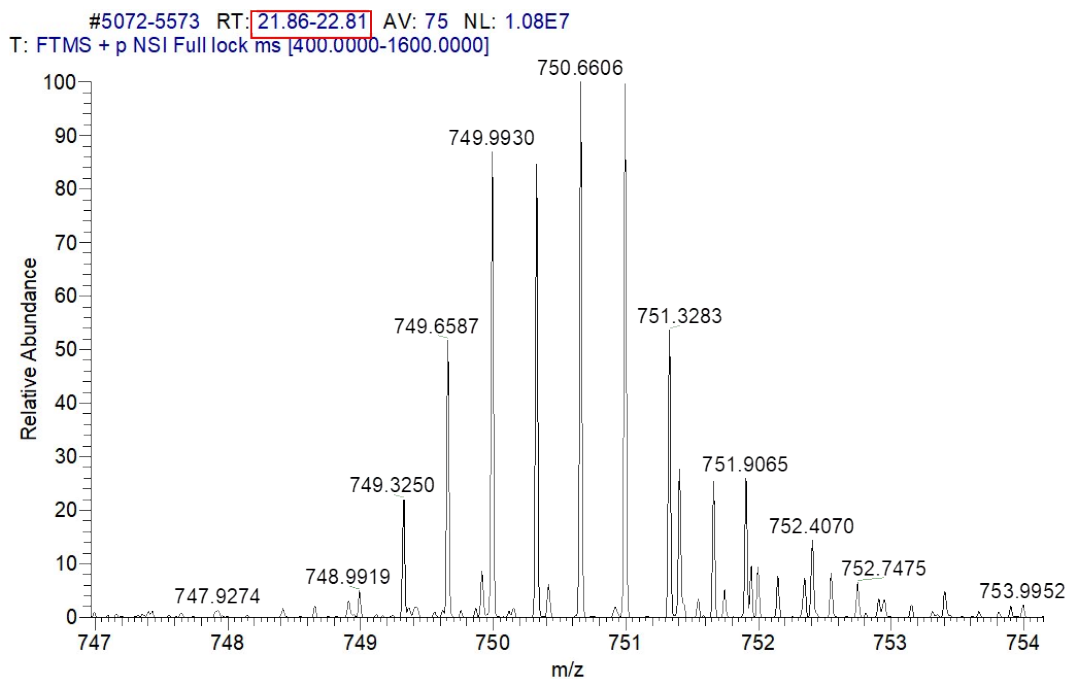


Figure S8: LC-MS analysis of Os<sup>II</sup>MPP Zoomed m/z 747-754 (RT 21-23 min)

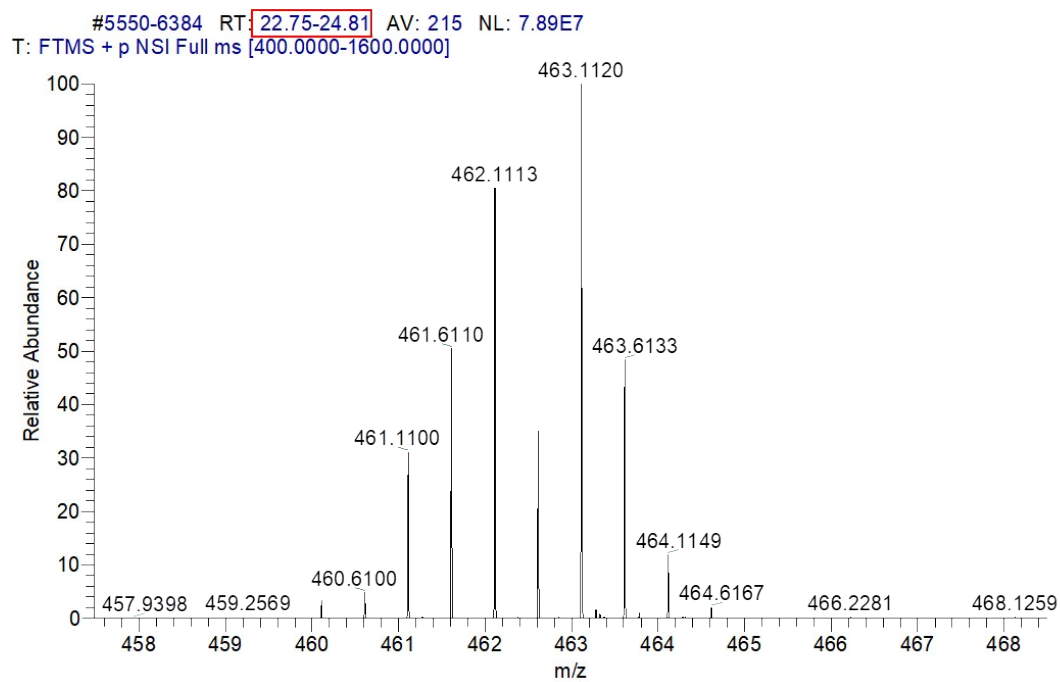


Figure S9: LC-MS analysis of Os<sup>III</sup>MPP Zoomed m/z 458-468 (RT 23-25 min)

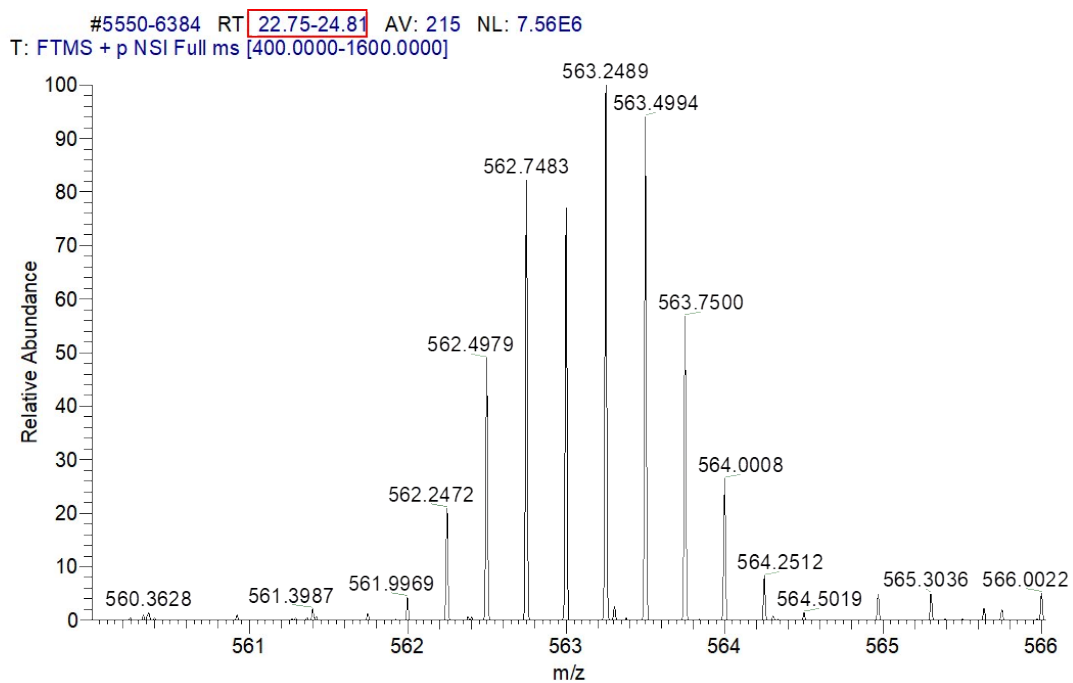


Figure S10: LC-MS analysis of Os<sup>III</sup>MPP Zoomed m/z 560-566 (RT 23-25 min)

HPLC Analysis of parent and conjugate Os(II) complex

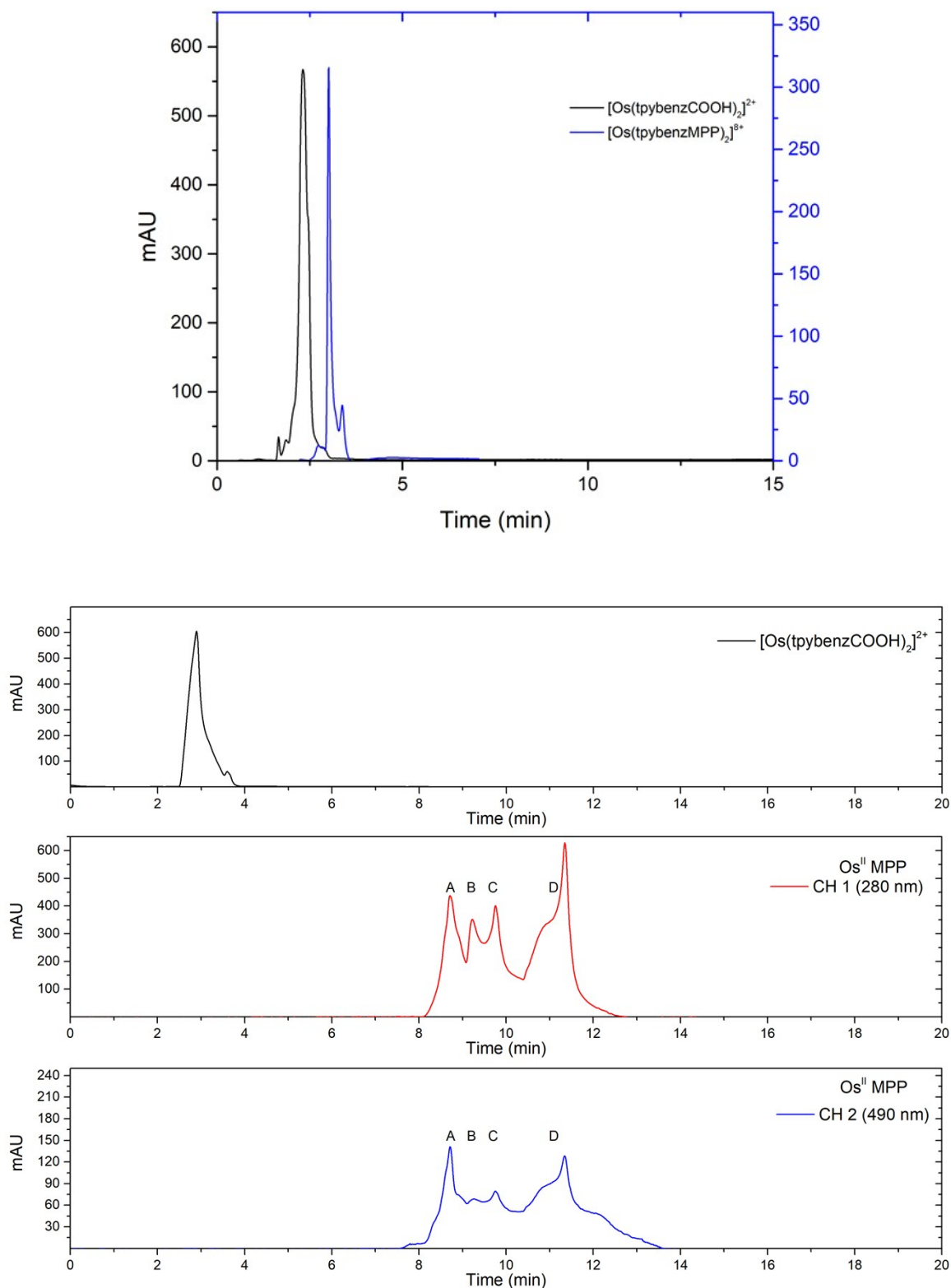


Figure S11: Top: HPLC Chromatogram of  $\text{Os}^{\text{II}}$  parent complex and  $\text{Os}^{\text{II}}$ MPP conjugate obtained RP-C18 HPLC with MeCN mobile phase. Bottom three traces show traces using gradient mobile phase detected at 280 nm. (Gradient MeCN/  $\text{H}_2\text{O}$  0.1% TFA gradient,  $1\text{ml min}^{-1}$ ). Elution of  $\text{Os}^{\text{II}}$ MPP conjugate at 8.3 min (Channel 1: 280 nm and Channel 2: 490nm). Diode array detection was used and the HPLC UV-vis spectrum of each peak was obtained during  $\text{Os}^{\text{II}}$  MPP analysis and is shown below.

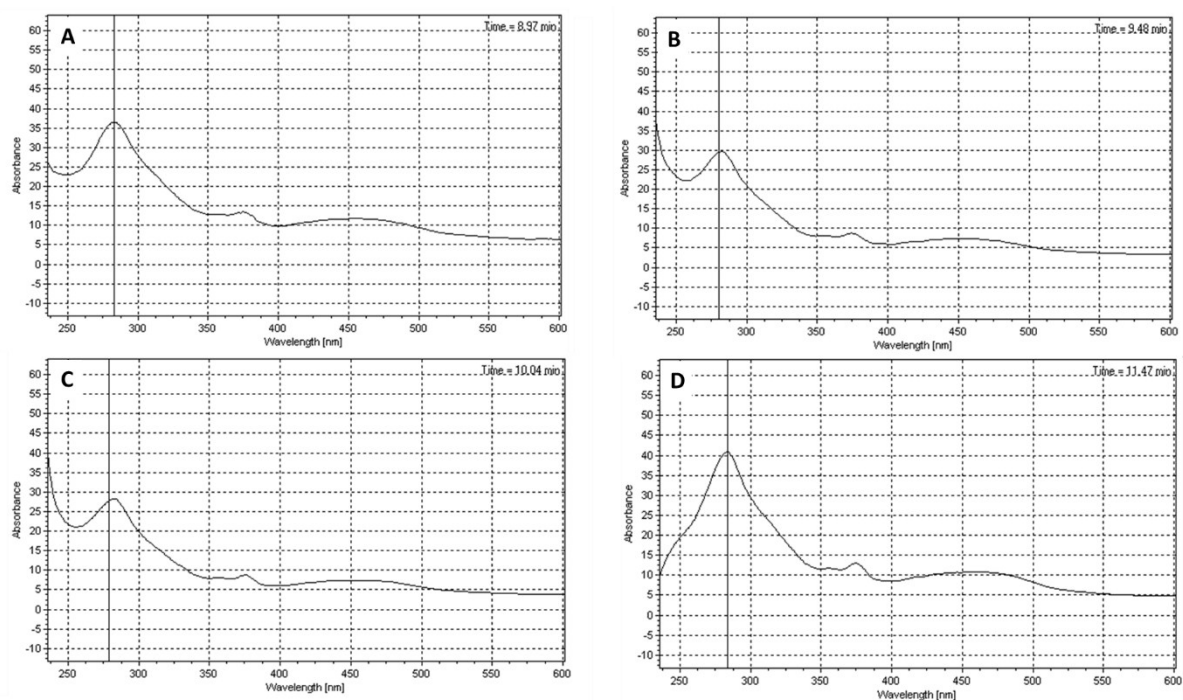


Figure S12: HPLC UV-vis spectra obtained for peaks observed during Os<sup>II</sup>MPP HPLC analysis illustrating the absence of a component with absorbance only in the UV-vis region as the MLCT band at a longer wavelength confirms Osmium-coordinated complex for each peak. The distribution of peaks in the conjugate product is suspected to originate from different ionization states of the conjugate.

### Spectroscopic Measurements of Os(II) parent complex and Os(II) conjugate

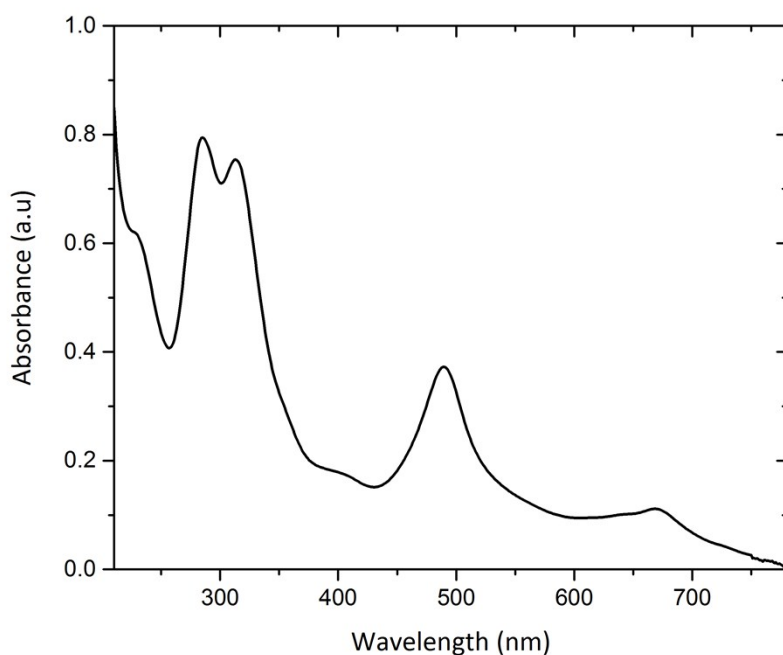


Figure S13: Absorbance spectrum of parent complex  $[\text{Os}(\text{tpybenzCOOH})_2]^{2+}$  **1** in acetonitrile solution (25  $\mu\text{M}$ ).

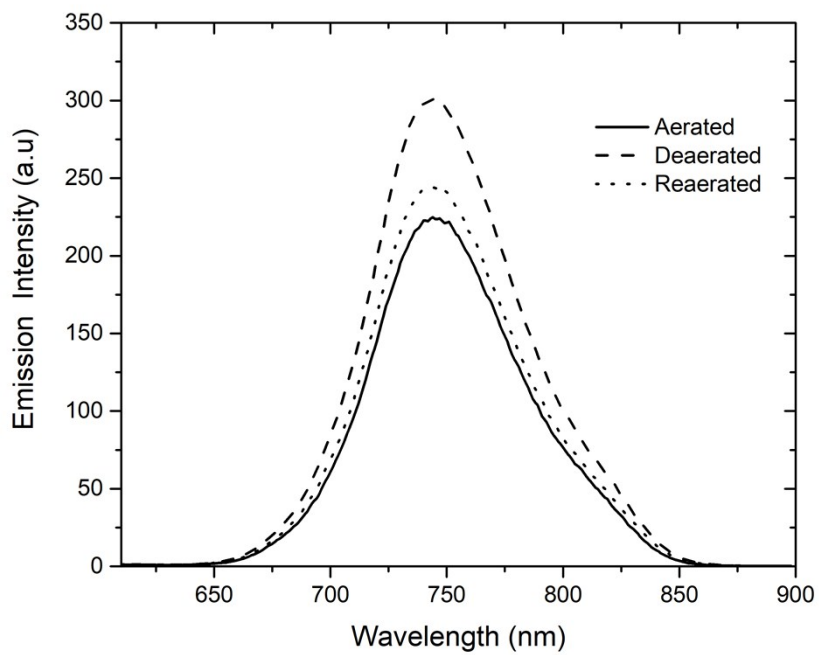


Figure S14: Emission spectra of parent complex  $[\text{Os}(\text{tpybenzCOOH})_2]^{2+}$  in acetonitrile (50  $\mu\text{M}$ ) under aerated and deaerated conditions (slit widths 10 nm / 10 nm). Solution was deaerated using nitrogen gas and oxygen concentration was measured using PreSense  $\text{O}_2$  sensor.

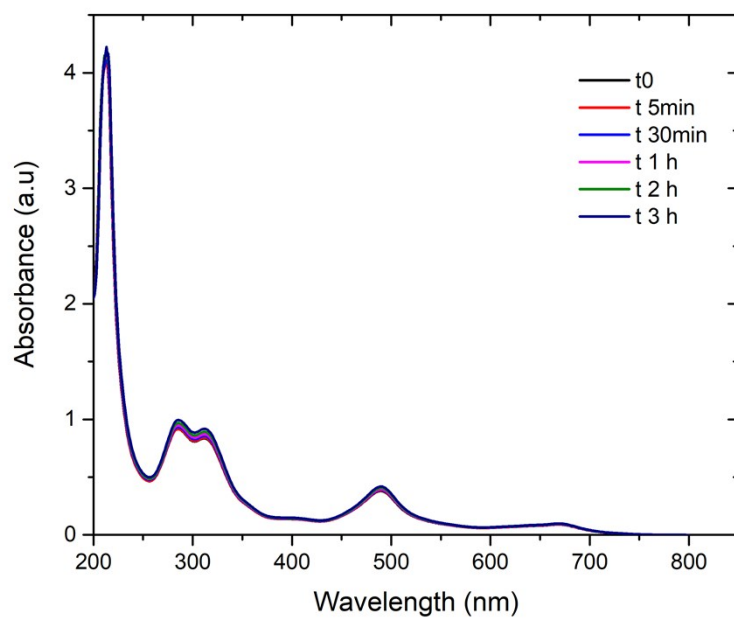
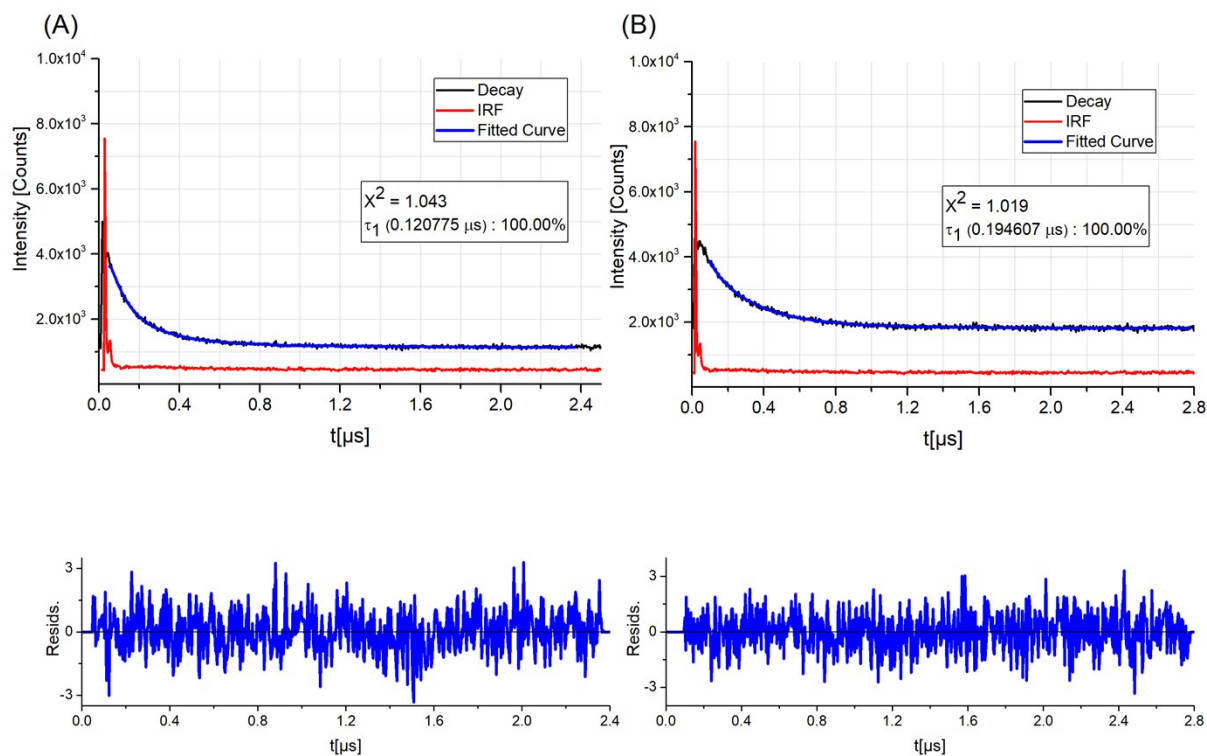


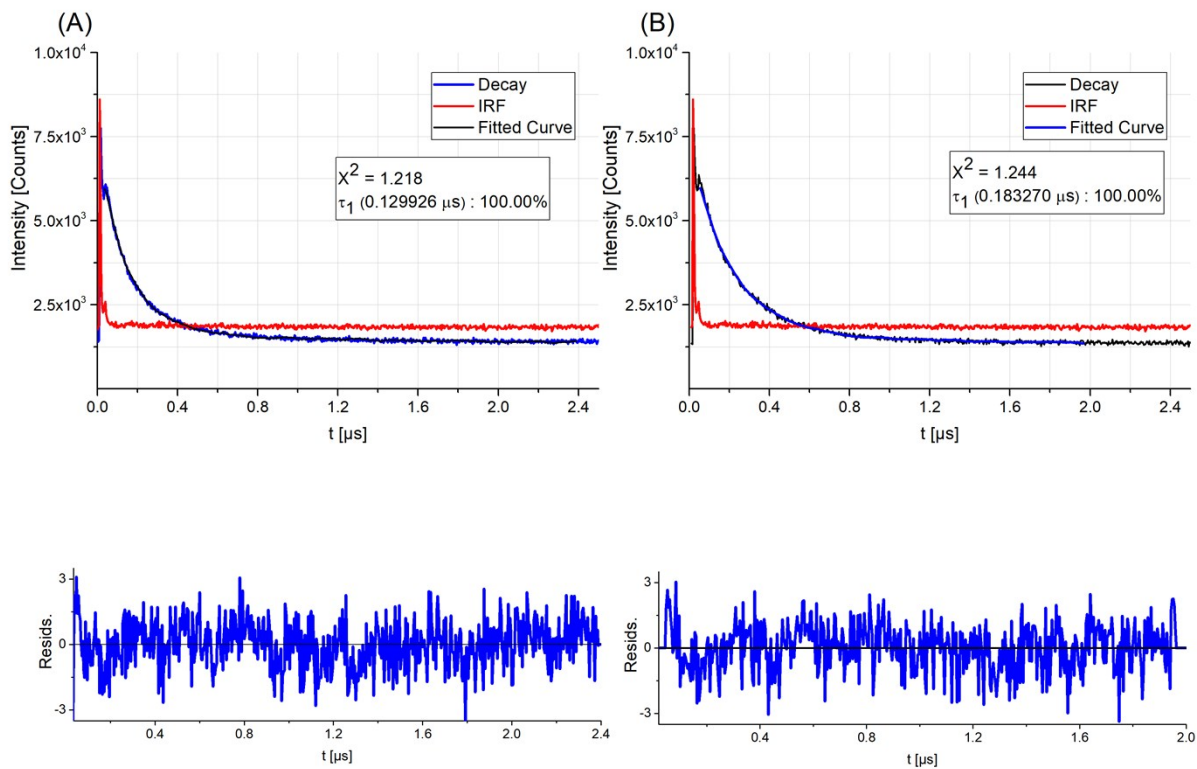
Figure S15: Absorbance spectra of parent complex  $[\text{Os}(\text{tpybenzCOOH})_2]^{2+}$  ( $50\mu\text{M}$ / PBS pH 7.4) following continuous photo-irradiation with ARC Lamp 150W for 3 h at Room Temperature.

Emission Decays of Os (II) parent and Os<sup>II</sup> MPP complex – Time- correlated single photon counting (TCSPC) measurements using NanoHarp 2.1, FluoTime100 (PicoQuant) and mono-exponentially fitted using PicoQuant Fluofit software.



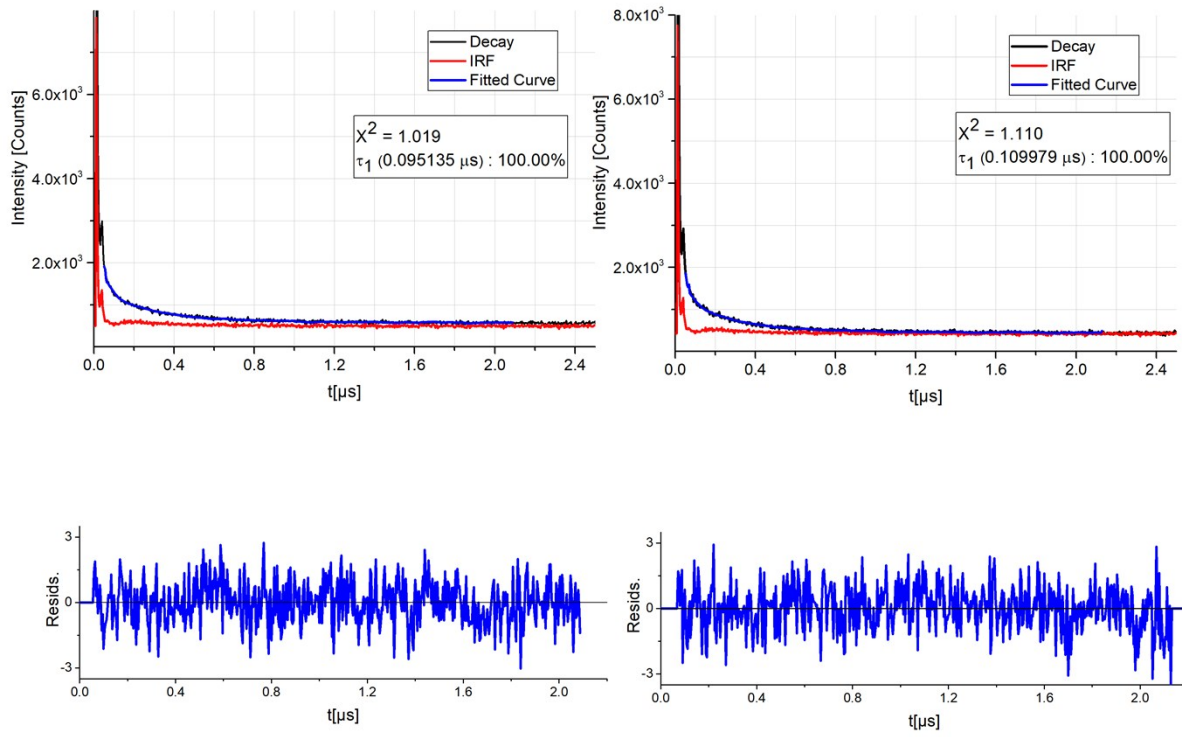
$$\int_{-\infty}^t IRF(t') \sum_{i=1}^x A_i e^{-\frac{t-t'}{\tau_1}} dt'$$

Figure S16: Emission Decays of parent complex  $[\text{Os}(\text{tpybenzCOOH})_2]^{2+}$  in aerated and deaerated acetonitrile (50 μM); Residual plots for the exponential fitting of both curves are shown below each plot.



$$\int_{-\infty}^t \text{IRF}(t') \sum_{i=1}^x A_i e^{-\frac{t-t'}{\tau_i}} dt'$$

Figure S17: Emission Decays of parent complex  $[\text{Os}(\text{tpybenzCOOH})_2]^{2+}$  in aerated and deaerated PBS pH 7.4 (50  $\mu\text{M}$ ); The residual plots for the exponential fitting of both curves are shown below.



$$\int_{-\infty}^t IRF(t') \sum_{i=1}^x A_i e^{-\frac{t-t'}{\tau_1}} dt'$$

Figure S18: Emission decay of conjugate Os<sup>II</sup> MPP under aerated and deaerated conditions (25 $\mu\text{M}$ / PBS pH 7.4); Residual Plots of the exponential fitting for both curves are shown below.

## Cytotoxicity Studies and determination of IC<sub>50</sub> of Os<sup>II</sup> MPP

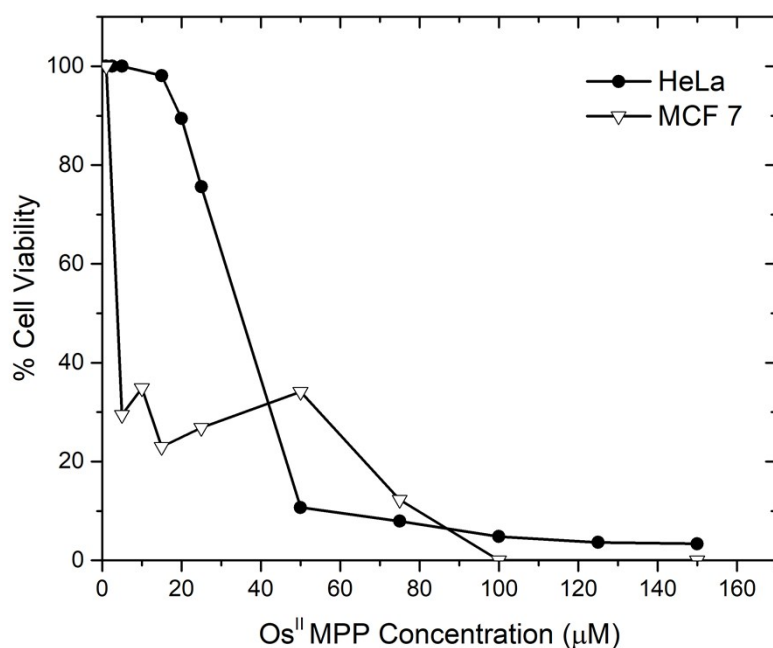


Figure S19: Cell Viability of HeLa and MCF 7 cells after 24hr exposure to Os<sup>II</sup> MPP probe. Live cells were treated with the probe followed by addition of Resazurin for 6 h. Absorbance was read at 570 nm with background at 600 nm subtracted (n=3).

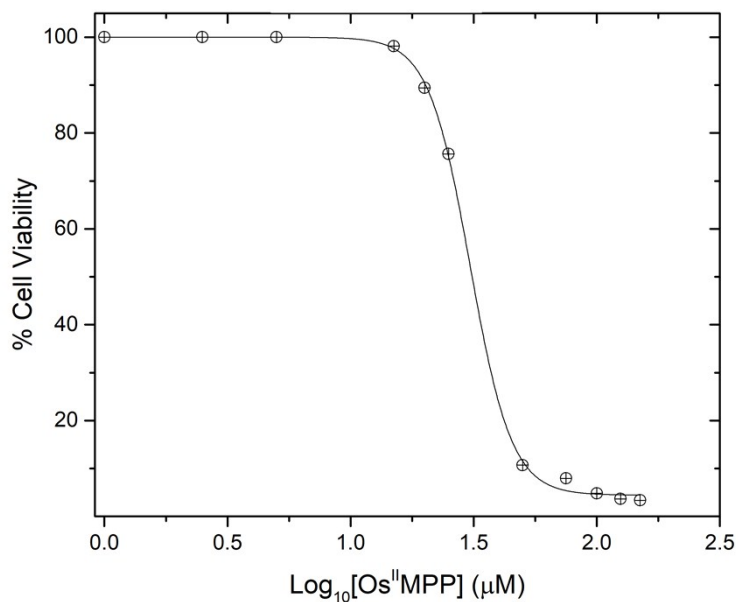


Figure S20: Determination of EC<sub>50</sub>. HeLa cells were incubated in the presence of Os<sup>II</sup> MPP (0.1µM to 150µM) for 24 h. Cell proliferation was assayed with Resazurin (n=3). The IC<sub>50</sub> value, the minimal amount of Os<sup>II</sup> MPP required to inhibit 50 % viability of HeLa cells was found to be 30.61µM.

## Confocal Imaging

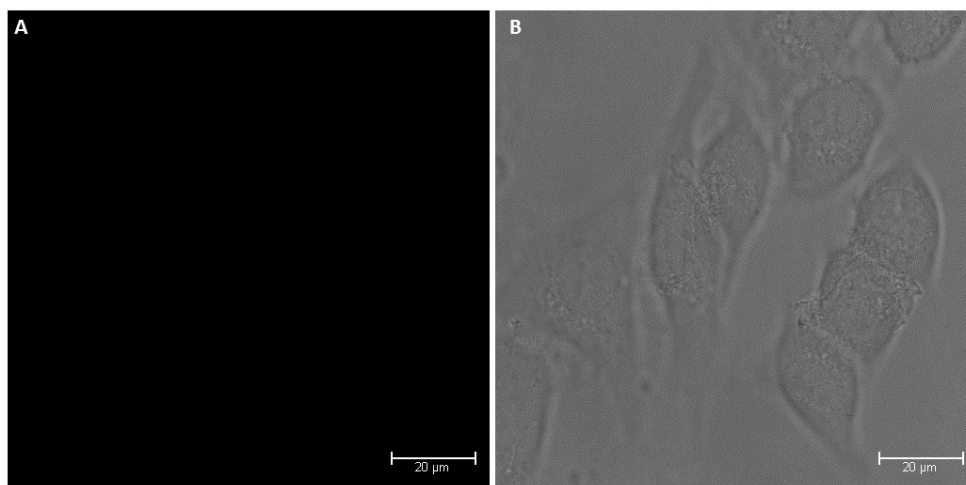


Figure S21: Confocal Imaging studies of  $[\text{Os}(\text{tpybenzCOOH})_2]^{2+}$ . Cells were treated with  $[\text{Os}(\text{tpybenzCOOH})_2]^{2+}$  at  $30\mu\text{M}$  for 2 h. (A) Osmium Channel: uptake of the parent complex was not evident; (B) Background channels showing HeLa cells. Cells were excited with 490 nm WLL and emission was collected between 650nm and 850 nm.

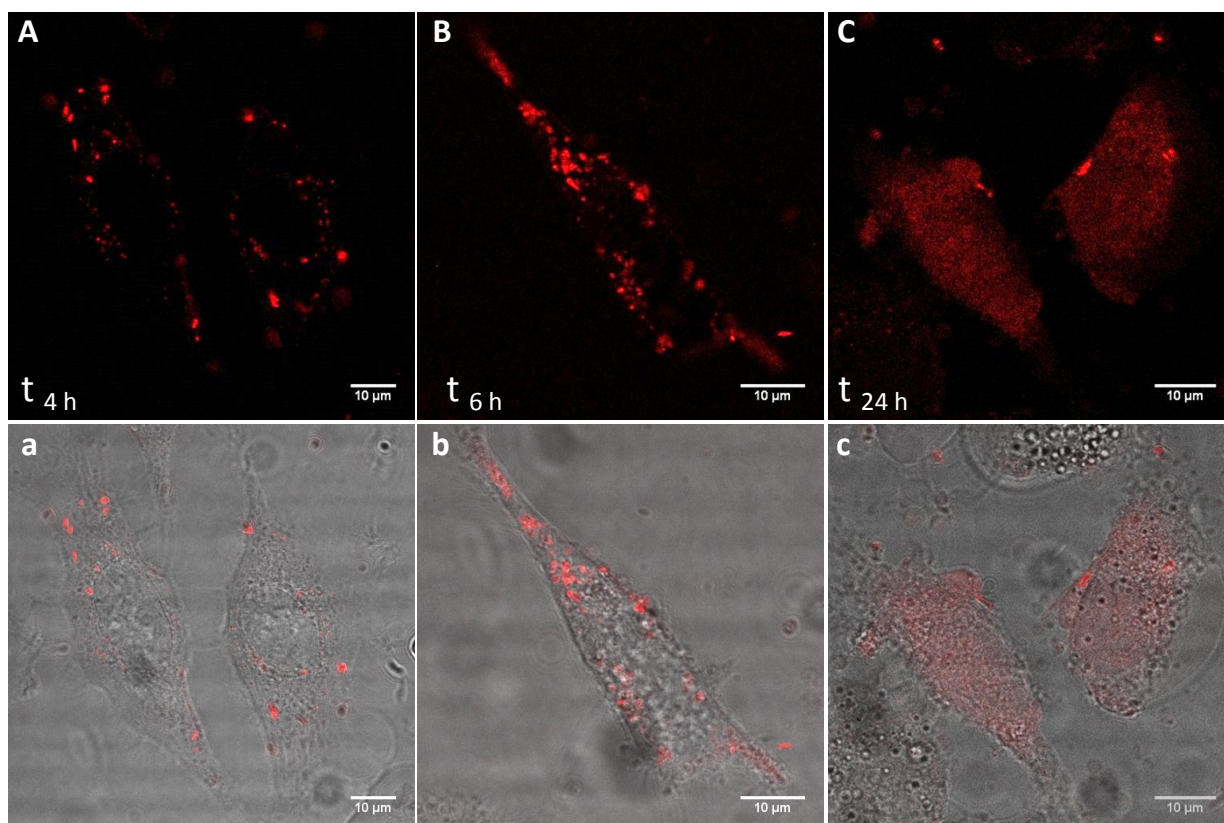


Figure S22: Confocal microscopy of HeLa cells incubated with  $\text{Os}^{\text{II}}$  MPP at  $30\mu\text{M}$  for (A) 4 h, (B) 6 h and (C) 24 h in cell media at  $37\text{ }^\circ\text{C}$  in the absence of light. (a-c) Overlay images with the background channel.  $\text{Os}^{\text{II}}$ MPP was excited using a 490 nm white light laser and emission was collected between 650nm and 850 nm.

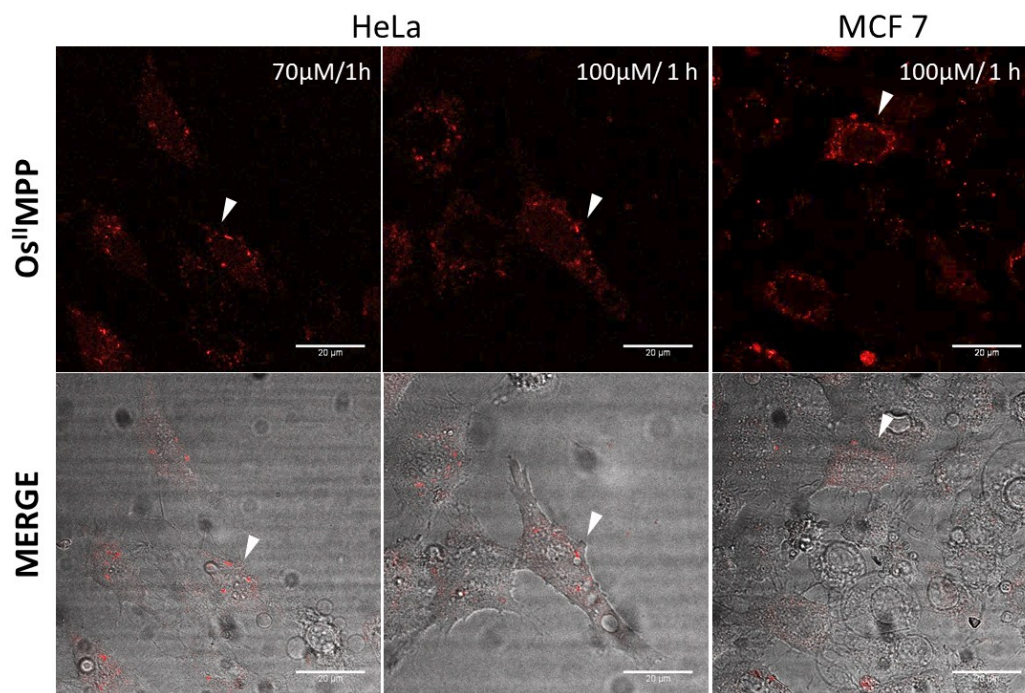


Figure S23: Confocal imaging of Os<sup>II</sup>MPP in HeLa and MCF 7 cells at increased concentrations; Uptake of Os<sup>II</sup>MPP probe is evident but changes are observed in the morphological features of cells indicative of cell death.

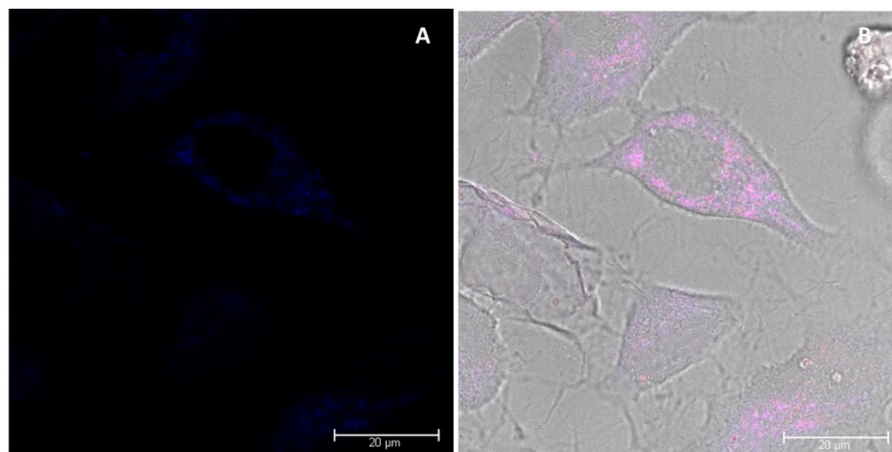


Figure S24: Co-staining with DRAQ7 following Os<sup>II</sup>MPP 30uM/2h; (A) Absence of nuclear staining confirms cells are viable; observed in blue is the emission of MitoTracker Deep Red due to co-excitation of MitoTracker Deep Red at 633 nm. (B) Overlay of all channels

## Polycaspase FAM-FLICA and MitoPT TMRE Assay

Table 1: MitoPT and FLICA Assay: Cell Population Experimental Conditions

Assay	Negative Control Populations	Positive Control Population	Experimental Populations
Mito PT	(1) Non-exposed population (2) DMSO (100 $\mu$ M/ 1 h)	CCCP (20 $\mu$ M/ 2 h)	Os <sup>II</sup> MPP 30 $\mu$ M/ 2 h Os <sup>II</sup> MPP 100 $\mu$ M/ 1 h
FLICA	(1) Non-exposed population (2) DMSO (100 $\mu$ M/ 1 h)	Staurosporine (1 $\mu$ M/ 3 h)	Os <sup>II</sup> MPP 30 $\mu$ M/ 2 h Os <sup>II</sup> MPP 100 $\mu$ M/ 1 h

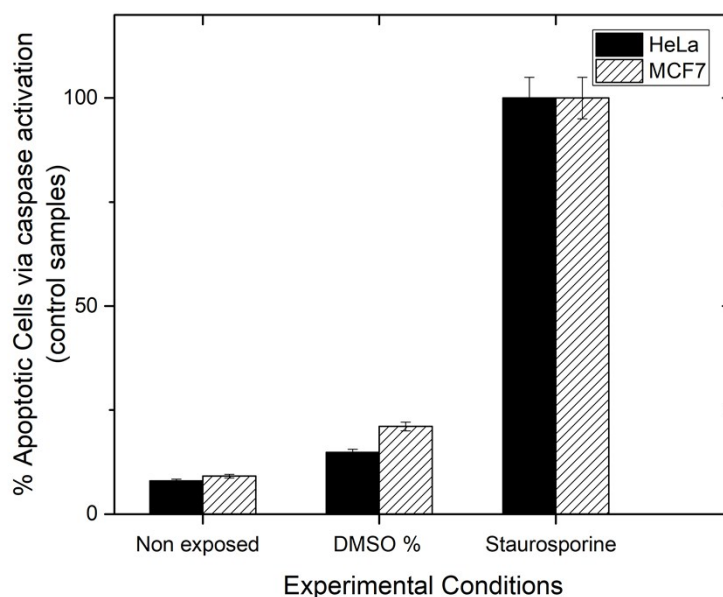


Figure S25: Control studies for the FLICA assay (n=3) in HeLa and MCF 7 cell line. Cells were cultivated at  $3 \times 10^5$  cells/well and were exposed to negative control 1 (non-treated) (B) negative control 2 DMSO (10% v/v) (C) positive control (staurosporine 1 $\mu$ M/ 3 h). Cells were spiked with 30X FAM-FLICA reagent (v/v ratio of 1:30) and incubated for 45 minutes at 37°C. Samples were analyzed in triplicate (3 x 100  $\mu$ l) in a black bottomed 96-well plate using Tecan Plate fluorescence plate reader set at 488 nm excitation and 520 nm emission.